International Journal of Civil Engineering

Geotechnical Engineering

Undrained triaxial shear behavior of grouted carbonate sands

M. Hassanlourad[1,*], H. Salehzadeh[2], H. Shahnazari[2]

Received: September 2009, Revised: November 2010, Accepted: May 2011

Abstract

The effects of cementation and the physical properties of grains on the shear behavior of grouted sands are investigated in this paper. The consolidated-undrained triaxial shear behavior of three grouted carbonate sands with different physical properties, including particle size distribution, particle shape and void ratio, was studied. Two sands were obtained from the north shores of the Persian Gulf, south of Iran, called Hormoz and Kish islands sands, and one sand was obtained from the south beaches of England and called Rock beach sand. The selected sands were grouted using a chemical grout of sodium silicate and tested after one month of curing. Test results showed that the effect of bonding on the shear behavior and strength depends on the bond strength and confining pressure. In addition, the shear behavior, yield strength and shear strength of grouted sands under constant conditions, including the initial relative density, bonds strength, confining pressure and loading, were affected by the physical properties of the sands. Furthermore, the parameters of the Mohr-Coulomb shear strength failure envelope, including the cohesion and internal friction angle of grouted sands under constant conditions, were affected by the physical properties and structure of the soils.

Keywords: Carbonate sands, Triaxial test, Grouting, Sodium silicate

1. Introduction

Carbonate sands are known as problematic soils. These soils have led to problems in civil projects, especially pile driving (API, 2000). In situ grouting of these soils can help to improve their weakness. Investigations on cemented carbonated sands showed the importance of improvement of these soils (e.g., Saxena and Lastrico (1978), Dupas and Pecker (1979), Clough and Sitar (1981), Allman and Poulos (1988), Huang and Airey (1988), Lade and Oveton (1989), Coop and Atkinson (1993), Salehzadeh et al. 2005, 2008 and Ismail et al., 2000 and 2002)). Also studies illustrated that the north shores of Persian Gulf and its islands contain such soils (Salehzadeh and Ghazanfari, 2004 and Hassanlourad et al , 2008.

Different cements like gypsum, Portland cement and calcite have been used for the cementation of carbonate sands in these studies (e.g., Ismail et al., 2000, 2002). Most of them used the mixing method for cementation. Ismail et al. (2000 and 2002) flushed the calcite through the sand particles to cement the carbonate sand.

In this research, the shear behavior of three carbonate sands was investigated using triaxial tests. The consolidated drained mechanical properties of these grouted and ungrouted carbonate sands were investigated, and the in situ improvement of carbonate sand was investigated by a model grouted micro pile (Hassanlourad et al. 2009 and 2010).

This research seeks to understand the consolidated undrained shear behavior, interaction of bonds and confining pressure using triaxial tests. Furthermore, the effect of the physical properties of the grains on the shear behavior and strength of grouted sands was studied under constant conditions, such as initial relative density, grout strength, confining pressure and loading rate.

2. Materials

Three types of carbonate sands were studied in this research. Two sands were obtained from the north of the Persian Gulf and one from a beach in the south of England, called Rock sand. The particle size distribution and microscopic images (SEM) of the sand types used in this research are illustrated in Figures 1 and 2, respectively. Figure 2 shows that Rock sand is finer than the others. Kish and Hormoz sands have similar particle size distributions with different grain shapes. Other physical properties of the sands used, such as particle specific

* *Corresponding Author: mhassanlourad@iust.ac.ir*
1 Faculty of Eng., Imam Khomeini International University, Qazvin, Iran
2 School of Civil Eng., Iran University of Science and Technology, Narmak, Tehran, Iran

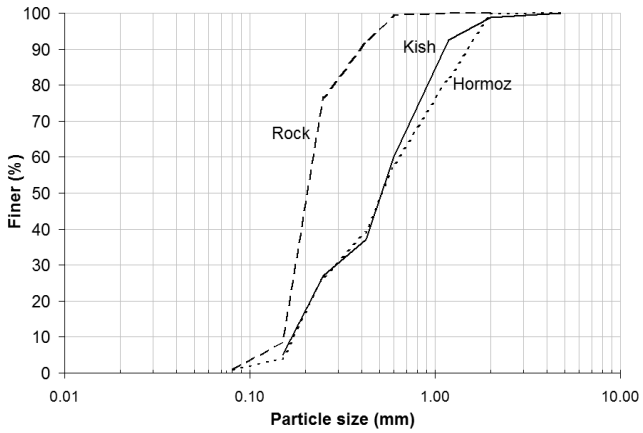

Fig. 1. Particle size distribution of sands

gravity, maximum and minimum void ratios, calcium carbonate content, uniformity coefficient (Cu), and particle shape, are summarized in Table 1.

The grout used for injecting the soil was a chemically based grout called sodium silicate ($Na_2O_2SiO_2$). The grout was produced by dissolving sodium silicate in water and adding two other chemical additives, formamide ($HCONH_2$) as a reactant and sodium aluminate ($NaAlO_2$) as an accelerator of the chemical reactions (EM 1110-1-3500, 1995). The characteristics of the grout used for injecting the sand samples are summarized in Table 2. The W/S ratio shown in this table represents the water to sodium aluminate ratio. The percentage of additives shown in Table 2 indicates the ratio of the weight of the additives to the weight of water plus sodium silicate.

3. Sample preparation and testing program

Specimens for triaxial tests were prepared in a loose condition with a relative density of 20% using the dry deposition method. Then, sodium silicate grout was injected into the samples at a low pressure of about 20 kPa. The grouted specimens were cylindrical, 40 mm in diameter and 83 mm in height. Figure 3 shows a schematic picture of the injection apparatus and grouted samples during the curing process in the molds. The ungrouted specimens were cylindrical and were 38 mm in diameter and 76 mm in height.

Unconfined compression tests showed that the rate of chemical reactions was different in sodium silicate grout for the different additive contents. However, the chemical reactions were almost complete within one month (Hassanlourad et al., 2009). Thus, it was decided to load the grouted samples after 28 days from the beginning of the curing time.

Samples were tested in the saturated state when they reached a B value of 0.95. After isotropic consolidation, samples were axially loaded under undrained conditions. The injected sands with weak and intermediate grout were loaded using a displacement-controlled method at a rate of 0.2 mm/min. Specimens with strong grout were loaded at a rate of 0.1 mm/min. In total, thirty tests were reported in detail (Table 3).

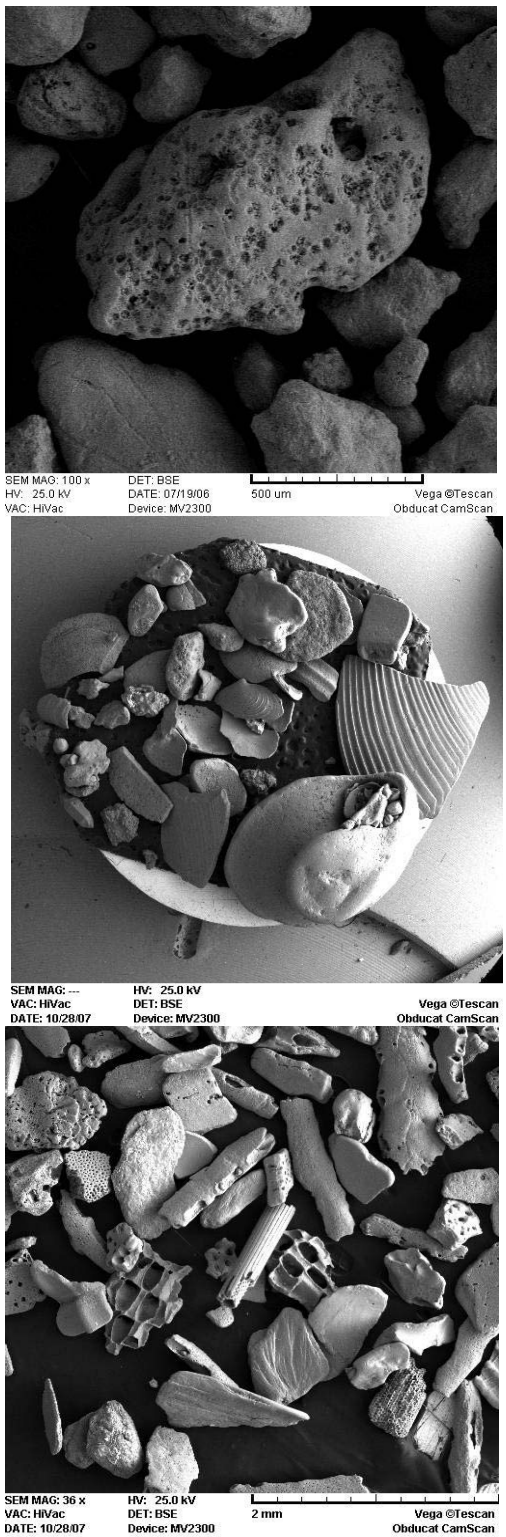

Fig. 2. SEM images of sands

3. Triaxial tests

Stress-strain and pore water pressure-strain behavior were studied using triaxial tests, and the effects of particles properties, confining pressure, bonds strength on the shear strength, yield and failure envelopes of grouted sands are discussed at the following sections.

Table 1. Physical properties of the sands studied

Sand	e_{min}	e_{max}	G_s	$CaCO_3$ (%)	Cu	Particle shape
Kish	0.50	0.71	2.6	93	3.	bulky, subangular and pa
Hormoz	0.643	0.975	2.70	75	3.6	platy, angular and some porous
Rock	0.838	1.473	2.72	90	1.5	needle- shaped, angular and porous

Table 2. Characteristics of the grouts used

Grout	W /S	$HCONH_2$ (%)	$NaAlO_2$ (%)	Remark
Weak	2	4	0.7	G1
Intermediate	1	5	1	G2
Stror	0.	6	1	G3

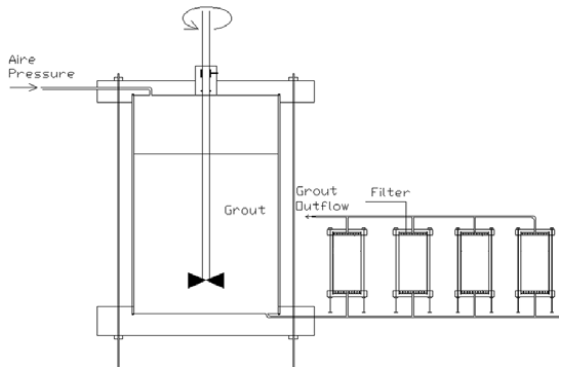

Fig. 3. Schematic picture of the apparatuses used for grouting

Table 3. List of the tests performed

Sand	State	Grout Strength	Dr (%)	σ_3' (kPa)	Code
Kish	ungrouted	-	20	100	KLCU100
				300	KLCU300
				50(	KLCU 50(
	grouted	Weak		100	KG1CU100
				300	KG1CU300
				50(	KG 1CU 50(
		Intermediate		0	KG2CU00
				100	KG2CU100
				300	KG2CU300
				50(	KG 2CU 50(
		Strong		100	KG3CU100
				300	KG3CU30(
				50(	KG 3CU 50(
Hormoz	ungrouted	-	20	100	HLCU100
				300	HLCU300
				500	HLCU500
	grouted	Intermediate		0	HG2CU00
				100	HG2CU100
				300	HG2CU300
				600	HG2CU500
Rock	ungrouted	-	20	100	RLCU100
				300	RLCU300
				600	RLCU600
			80	100	RDCU100
				300	RDCU300
				500	RDCU500
	grouted	intermediate	20	0	RG2CU00
				100	RG2CU100
				30(	RG 2CU 30(
				500	RG2CU500

4. Triaxial stress-strain behavior

Isotropic consolidated undrained triaxial test results for the ungrouted and grouted sands are demonstrated in Figures 4 to 6, as deviatoric stress and pore water pressure versus axial strain and stress path.

The stress-strain curves of all grouted samples show an initial linear part and then a yield point at axial strains of about 1%, which demonstrates the fracturing of the bonds. The stress-strain behaviors of weakly grouted (G1) and ungrouted Kish sand were similar, and the bonds had little effect on it. The effect of the bonds was only considerable up to an axial strain of about 1-1.5% and, beyond that, dissipated gradually with increasing axial strain (Figure 4a).

The peak strength (failure point) of the Kish sand samples grouted with intermediate grout (G2) developed after the yield point and at axial strains of about (7-15)%, depending on the confining pressure (Figure 4). The strength of these samples included two components: internal friction and bond resistance. The bond resistance decreased after the peak point because of additional fracture, such that the stress-strain curves of the ungrouted and grouted samples converged on each other at the end of the test at axial strains of about 20%. The difference of the strength at the end of loading was due to the greater negative pore water pressure of the grouted samples compared to the ungrouted samples (Figure 4).

The yield strength of Kish samples grouted with strong grout (G3) was also their peak strength (Figure 4). Thus, the bond strength was higher than the internal friction resistance in these samples. After the yield point, increasing the negative pore water pressure prevented the rapid decrease of the strength up to axial strains of about 4-5% (Figure 4). The rate of strength reduction was intensified with greater fracture of the bonds. These samples failed brittle with the shear band formation in the samples up to applied confining pressures of 500 KPa.

5. Pore water pressure built up and stress path

As shown in Figures 4b to 6b, bonding the particles to each other changes the pore water pressure built up rate. In weakly (G1) and intermediate (G2) grouted samples for all confining pressures, the positive and negative pore water pressures were lower and higher than those of the ungrouted samples, respectively. However, this trend was sometimes displaced in weakly grouted samples. In strongly grouted samples, both the positive and negative pore water pressures at all confining pressures were more than those of the ungrouted samples (Figure. 4b).

The stress path of tested samples was based on definition of q and p' parameters (Eq. 1), and they are shown in Figures 4c to 6c.

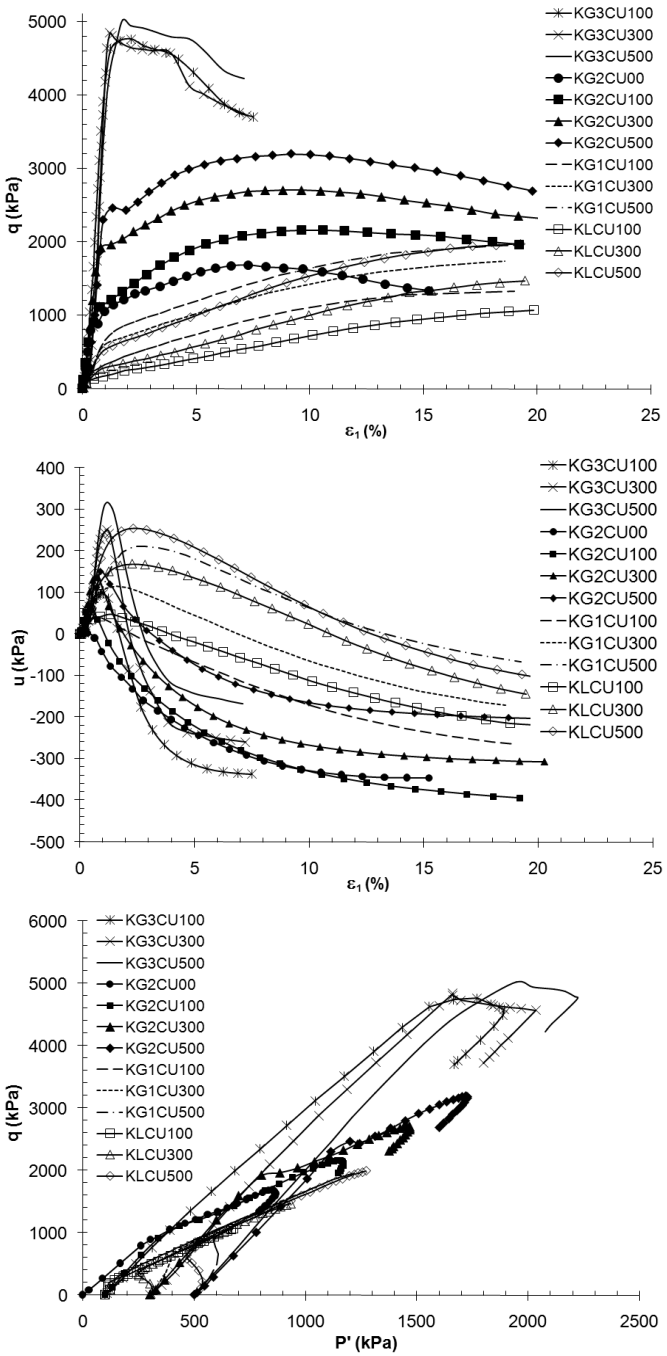

Fig. 4. Grouted Kish sand shear behavior, (a) deviatoric stress versus axial strain, (b) pore water pressure versus axial strain and (c) stress path

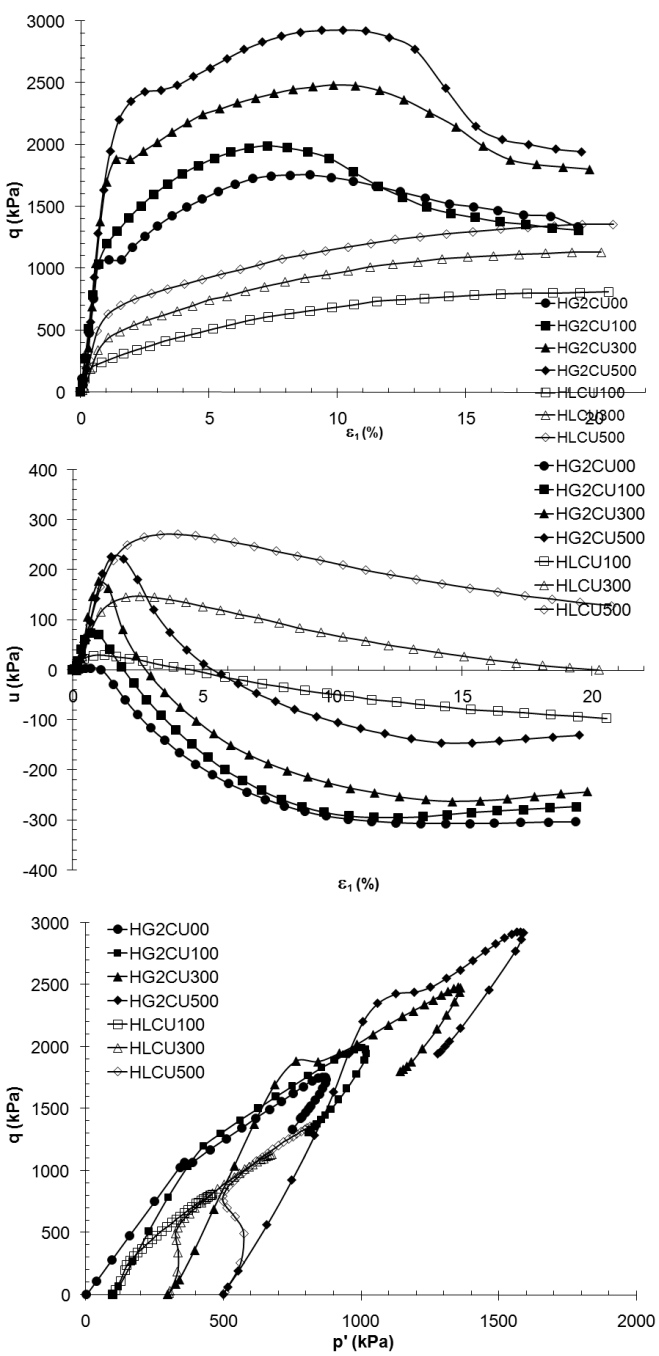

Fig. 5. Grouted Hormoz sand shear behavior, (a) deviatoric stress versus axial strain, (b) pore water pressure versus axial strain and (c) stress path

$$q = \sigma_1' - \sigma_3'$$
$$p' = \frac{\sigma_1' + 2\sigma_3'}{3} \quad (1)$$

Graphs of q-p' show that bonding the grains elongated the stress path and increased both the q and p' parameters. In other words, undrained shear strength of the grouted sands was higher than that of the drained shear strength. Saxena and Lastrico (1978) and Ismail et al. (2002) reported this behavior for cemented carbonate sands with Portland cement.

6. Effect of soil particles properties

Figure 7 compares the stress-strain behavior, pore water pressure, principal stresses ratio, yield and failure strength of the Kish, Hormoz and Rock grouted carbonate sands with intermediate grout (G2), which behaved differently and showed the effect of the physical properties of particles on the shear behavior of grouted soils.

The stress-strain curves of the ungrouted sands were also different; nevertheless, bonding the grains intensified the difference. Kish sand showed the maximum shear strength

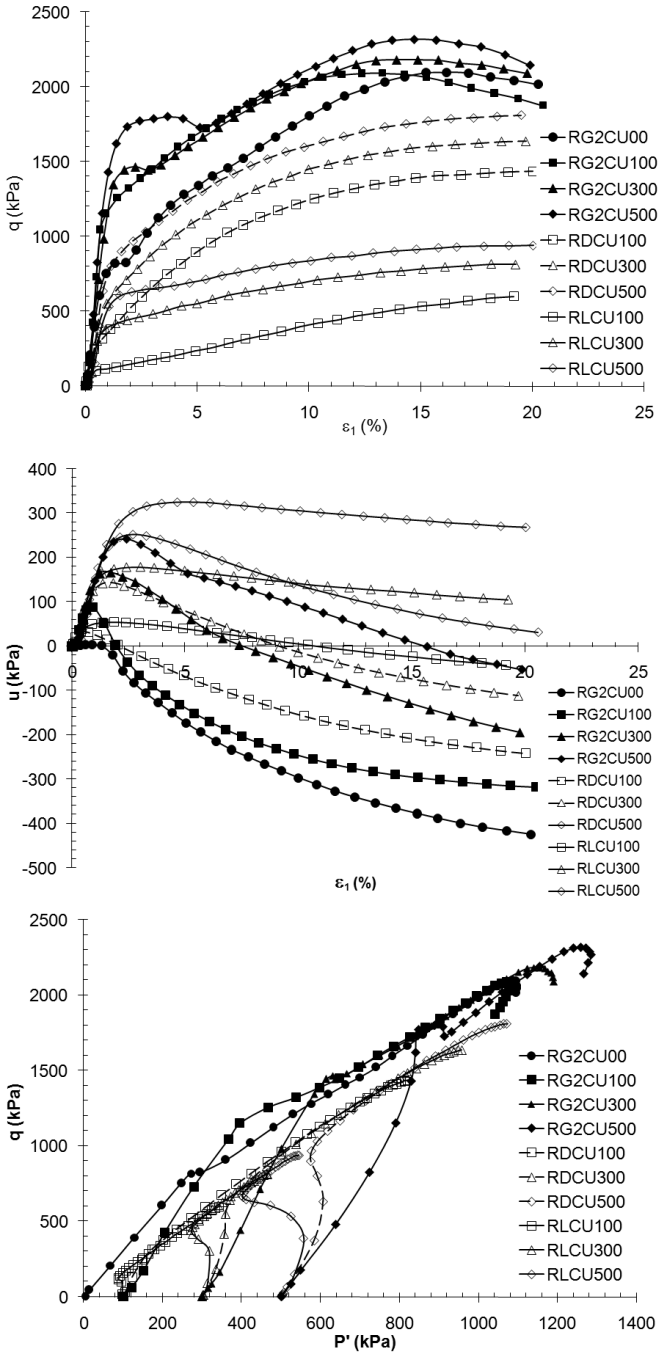

Fig. 6. Grouted Rock sand shear behavior, (a) deviatoric stress versus axial strain, (b) pore water pressure versus axial strain and (c) stress path

both in the ungrouted and grouted states (Figures 4a, 6a and 7). All three grouted sands showed a similar ductile stress-strain behavior under both 100 kPa and 500 kPa. Nevertheless, increasing the confining pressure increased the yield step (the horizontal part after the yield point) differently for the three grouted sands, which revealed that the effects of bonds and the physical properties of the grains were dominant at low and high confining pressures.

Different rates and values of the pore water pressure after the yield point and bonds fracturing for the three grouted sands showed the effects of the physical properties of the particles, including particle size distribution and shape.

Figure 7 shows that the difference in the principal stress ratio was high at the beginning of loading, and increasing the axial strain caused them to converge on each other. This difference was greater at a confining pressure of 100 kPa compared to 500 kPa. Therefore, the effect of the physical properties of the particles is important under low confining pressures. The yield strength of grouted sands under a confining pressure of 500 kPa was little affected by the physical properties of the particles compared to 100 kPa.

Increasing the axial strains decreased the principal stress ratio because of the fracturing of the bonds and the resulting reduction in cohesion. Beyond an axial strain of about 1%, the effect of the physical properties of the particles was considerable on the shear behavior and strength, and a large number of bonds were fractured (yield point).

7. Effect of confining pressure on the shear strength

The ratios of the yield and peak strength to the unconfined compression strength (q_y/q_{uc} and q_{max}/q_{uc} , respectively) for the grouted sands with intermediate grout are illustrated in Figures 8 and 9, respectively, versus the confining pressure. The ratios of q_y/q_{uc} and q_{max}/q_{uc} increased differently with increasing confining pressures.

The confining pressure has the maximum and minimum effects on the both yield and failure strengths of Rock and Hormoz grouted sands, respectively (Figures 8 and 9). The effects of the confining pressure on the yield and peak strengths of Kish sand were between those of the other two soils. In other words, the cohesions of grouted Hormoz and Rock sands resulting from bonds were the highest and lowest, respectively, which reveals the effect of the physical properties of grains on the mechanical properties of the grouted sands.

The increase of the peak strength of the grouted sands with confining pressure was expected because of the increase in the internal fiction resistance, and the internal friction resistance was the main factor behind the increase due to the fracture of a large number of bonds up to the peak point. The high negative pore water pressure development in the grouted samples increased the peak shear strength, and growing the bond crystals on the particles intensified the dilation of the soil.

Ismail et al. (2002) cemented RT carbonate sand using three cements of Portland cement, gypsum and calcite, and revealed that the yield strengths of the gypsum and calcite cemented samples were only slightly affected by the confining pressure. Coop and Atkinson (1993) reported the small effect of the confining pressure on the yield point for Dog's Bay cemented carbonate sand using gypsum. In addition, Ismail et al. (2002) stated that the effect of the confining pressure on the yield point of carbonate sand cemented by Portland cement was considerable. Therefore, the effect of the confining pressure on the yield point is a function of the physical properties of the soil and the cement type.

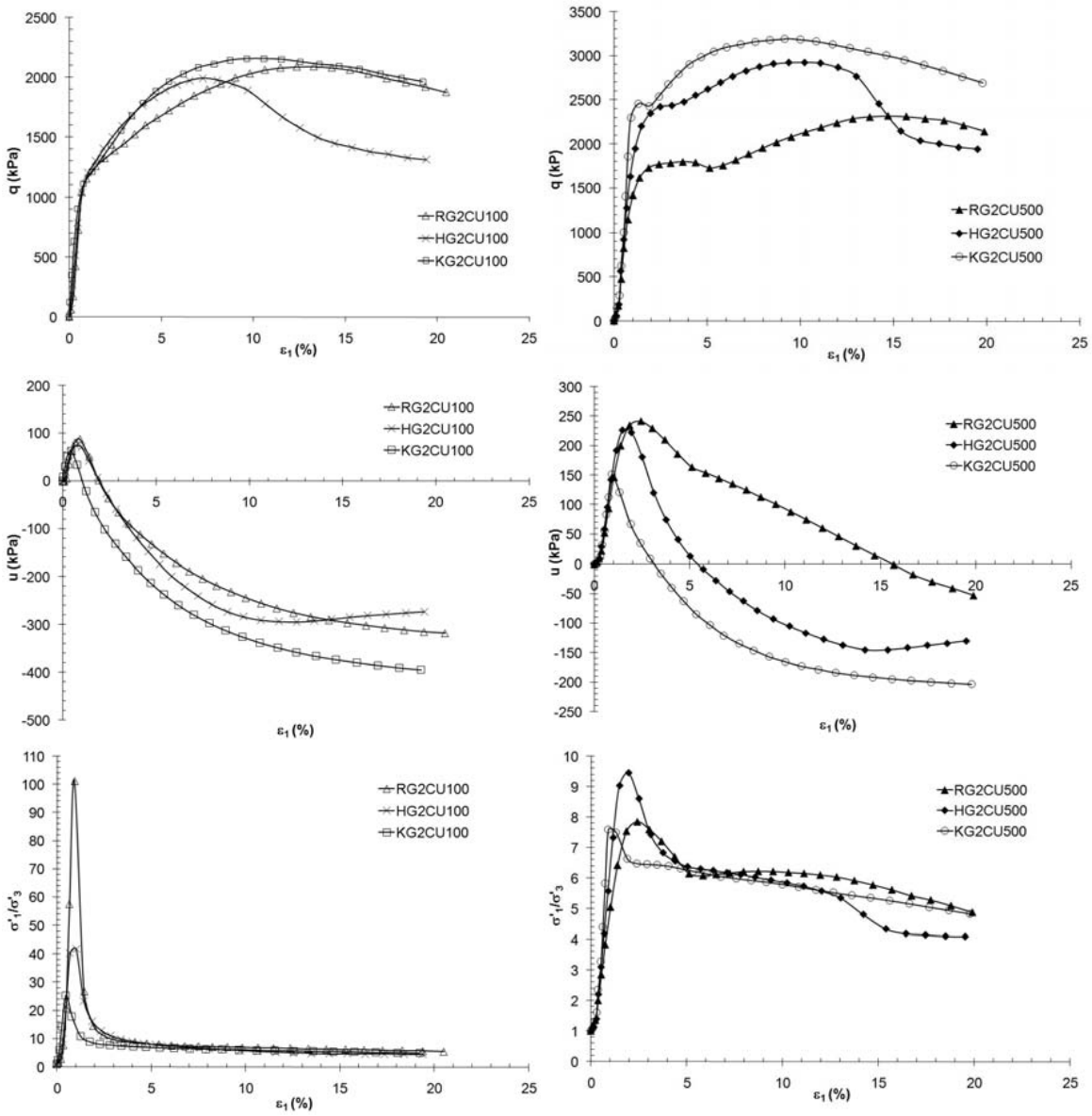

Fig. 7. (a) Deviatoric stress, (b) pore water pressure and (c) principal stresses ratio versus axial strain of grouted sands under confining pressures of 100 and 500 kPa

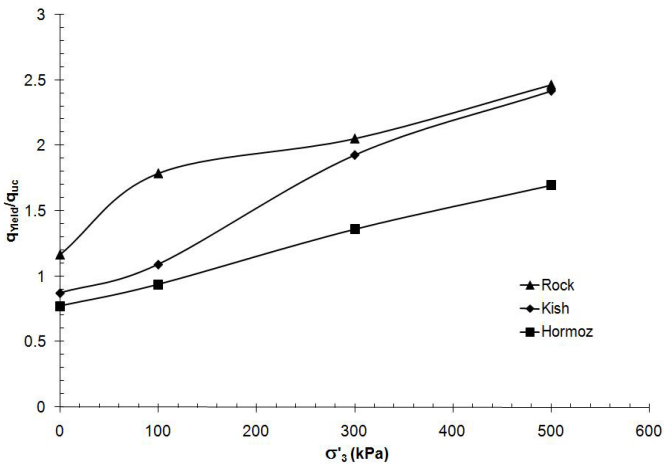

Fig. 8. Yield strength to unconfined compression strength ratio versus confining pressure

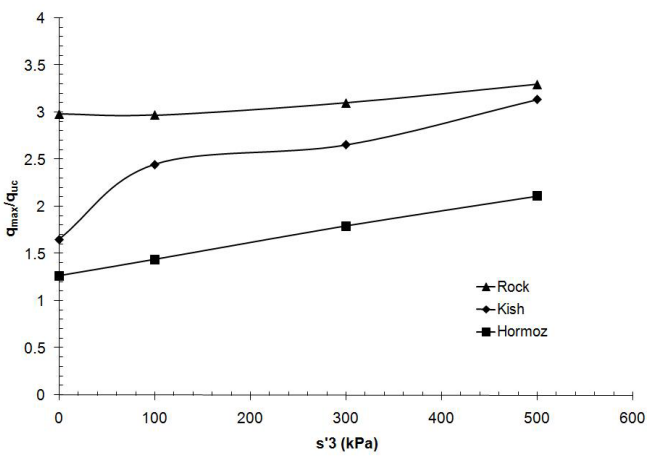

Fig. 9. Peak strength to unconfined compression strength ratio versus confining pressure

8. Effect of bonds on the shear strength

The ratio of q/p' at the phase transformation point (that is yield point too) is demonstrated in Figure 10 for both the ungrouted and grouted states with intermediate grout. This figure shows that bonding the particles increases the average of q/p' ratio from 1.6 (at σ'_3=*100kpa*) to 1.3 (at σ'_3=*500kpa*). Vaid and Chern (1988) revealed that cumulative strains remain small until the stress path passes the phase transformation line during cyclic loading. Ismail et al. (2002) also reported such a trend for RT carbonate sand cemented using Portland cement. Sharma and Ismail (2006) demonstrated that pore water pressure and strains increase rapidly under cyclic stress ratios greater than the phase transformation stress ratio for Good-Wyn and Ledge-Point carbonate sands. Therefore, increasing the q/p' at phase transformation ratio increases the cyclic resistance.

Figure 11 shows that bonding the grains increases the average of maximum principal stress ratio (σ'_1/σ'_3) from 1.51 (at σ'_3=*100kpa*) to 1.26 (at σ'_3=*500kpa*). The lower increase in the maximum principal stress ratio in comparison with increment of phase transformation point stresses ratio (q/p') is related to greater fracture of the bonds up to the peak point. Therefore, the shear strength of grouted soil has two components of cohesion resulting from bonds and internal friction resistance, in which increasing the confining pressure reduces the cohesion and increases the friction component. Figure 11 reveals that bonding the particles has the highest and lowest effect on Kish and Rock sands, respectively, showing their different bonding potentials. The particle size distribution of Kish and Rock sands are wide and uniform, respectively. However, Rock sand is finer than Kish sand.

9. Yield and failure envelope of grouted sands

The Mohr-Coulomb failure envelope is defined based on the effective stresses as follows:

$$\tau = c' + \sigma'_n \tan\varphi' \qquad (2)$$

The equivalent Mohr-Coulomb Yield and failure envelope of grouted sands with intermediate grout and its parameters (c' and ϕ') are demonstrated in Figure 12 and Table 4, respectively. This relationship is able to predict the yield and failure strength of the grouted soils.

The effective cohesion and internal friction angle parameters of the yield envelope for the Kish, Hormoz and Rock sands were about 353, 424 and 300 kPa and 35°, 32.5° and 33°, respectively. The effective cohesion and internal friction angle parameters of failure envelope for the Kish, Hormoz and Rock sands were about 194, 175 and 164 kPa and 38.5°, 40° and 40.2°, respectively. The average effective internal friction angle of the Kish, Hormoz and Rock sands was about 43.4°, 43.5° and 43.3°, respectively. The failure internal friction angle of the grouted sands was lower than that of the ungrouted sand, probably because of a thin layer of grout that covered the grains and then reduced the friction.

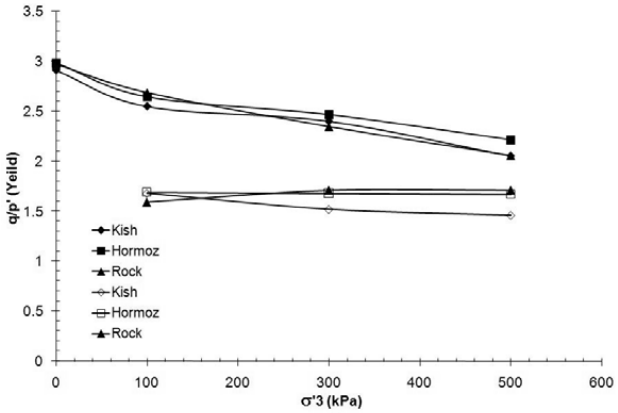

Fig. 10. q/p' at PT (yield) point versus confining pressure

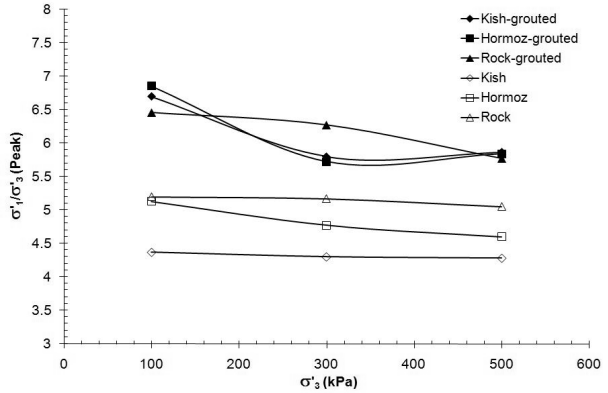

Fig. 11. q/p' at the peak point versus confining pressure

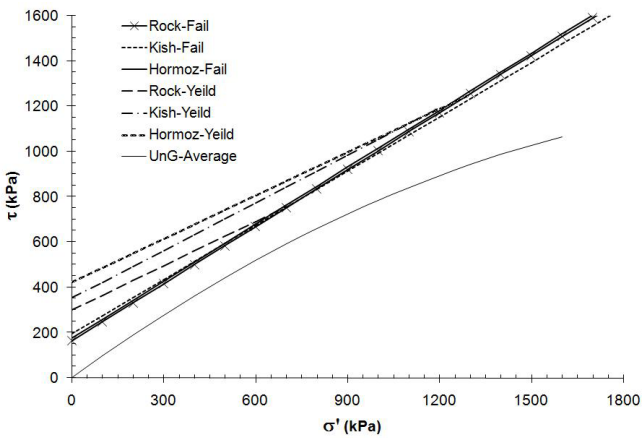

Fig. 12. Mohr -Coulomb yield and failure envelopes of the grouted sands

Table 4. Parameters of the Mohr-Coulomb yield and failure envelope

Soil	State	Envelope	c' (kPa)	φ' (Deg)
Kish	Ungrouted	Failure	-	43.4
Hormoz			-	43.5
Rock			-	43.
Kish	Grouted	Yield	353	35
Hormoz			424	32.5
Rock			300	33
Kish		Failure	194	38.5
Hormoz			175	40
Rock			164	40.

Allman and Poulos (1988) and Coop and Atkinson (1993) stated that the internal friction angle was slightly reduced by the cement percent. In contrast, Markou and Atmatzidis (2002) stated that grouting a siliceous sand using a kind of Fly Ash showed that the internal friction angle of the grouted sand is higher than that of the ungrouted state. Dano et al. (2004) grouted four siliceous sands with a very fine Portland cement and reported the same internal friction angle for both the grouted and ungrouted sands. Clough and Sitar (1981) reported the same for naturally cemented sands. Notably, the soils studied in this research were carbonate sands with a higher internal friction angle in comparison with siliceous sands (Golightly and Hyde, 1988; Hull et al. 1988). The effect of the bonds on the internal friction angle is complex and depends on the soil and cement type. However, the higher internal friction angle of the grouted soil in comparison with ungrouted soil is related to the limitation of the particle movement due to the cohesion produced (Markou and Atmatzidis, 2002). Equating the grouted and ungrouted internal friction angle is related to the lack of disturbance of the soil structure because of the low grouting pressure (Comberfort, 1979).

10. Conclusions

Generally, the grouting and bonding of grains improve the shear strength of sands. However, the improvement potential of soil depends on different factors. Triaxial tests performed on three different carbonate sands revealed the followings:

1. Weak bonding has no significant effect on the shear behavior, so that the internal friction between the grains is the main factor for the grouted soil strength.

2. At intermediate bonding, both the internal friction and cohesion resulting from bonds affect the shear behavior and strength of the grouted sand. In other words, the yield and failure shear strength of grouted sands are a function of both the internal friction and cohesion resulting from particle bonding. A portion of each depends on the confining pressure and physical properties of the sand physical.

3. With strong bonding, the shear behavior and shear strength of grouted sand only depends on the bond resistance (up to a confining pressure of 500 kPa), and the internal friction has no considerable effect. However, the internal friction is effective after the yielding of bonds or yield point.

4. The shear behavior and shear strength of grouted sands under the same conditions, including initial relative density, grout strength, confining pressure and loading rate, are affected by soil physical properties like particle size distribution, shape of grains, void ratio and soil structure.

5. The Mohr-Coulomb shear failure envelope is able to predict the yield and failure shear strength of grouted sands. The yield (bonds fracturing) strength of grouted sand is the shear failure strength at low effective normal stress. Nevertheless, the shear failure strength became higher than the yield strength with increasing effective normal stress and decreasing bond resistance, in comparison with internal friction resistance. Three separate shear yield and failure envelopes with different cohesion and internal friction angle were observed for the three sands grouted with the same grout.

References

[1] Airey, D.W. (1993), "Triaxial Testing of Naturally Cemented Carbonate Soil", Journal of Geotechnical and Geoenviromental Engineering, ASCE, Vol. 119, No.9, pp. 1379-1398.

[2] Allman, M.A., and Poulos, H.G. (1988), "Stress-Strain Behavior of an Artificially Cemented Calcareous Soil", Proceeding of lst International Conference on Calcareous Sediments, Perch, Australia. Vol. 1, pp. 51-60.

[3] API (2000), "Recommended Practice for Planning, Designing and Constructing Fixed Offshore Platforms", American Petroleum Institute, API RP-2A.

[4] Clough, G. W., and Sitar, B. (1981). "Cemented Sands under Static Loading", Journal of Geotechnical and Geoenvironmental Engineering, Div., Am. Soc. Civ. Eng., Vol. 107, No. 6, pp. 799-817.

[5] Coop, M.R. and Atkinson, J.H. (1993), "The Mechanics of Cemented Carbonate Sands", Geotechnique, Vol. 43, No. 1, pp. 53-67.

[6] Dano, C., Hicher, P.-Y., and Tailliez, S. (2004), "Engineering Properties of Grouted Sands", Journal of Geotechnical and Geoenvironmental Engineering, ASCE, Vol. 130 No. 3, pp. 328-338.

[7] Dupas, J. M., and Pecker, A. (1979), "Static and Dynamic Properties of Sand-Cement.", Journal of Geotechnical and Geoenvironmental Engineering, ASCE, Vol. 105 No. 3, pp. 4198-436.

[8] Hassanlourad, M , Salehzadeh H. and Shahnazari H. (2008) " Dilation and particle breakage effects on the shear strength of calcareous sands based on energy aspects", International Journal of Civil Engineering, Vol. 6, No. 2 , pp. 108-119.

[9] Hassanlourad, M., Salehzadeh, H. and Shahnazari H. (2009), "Improvement of Calcareous Sand by Chemical Grouting", Amir Kbir University Journal (in Farsi), Vol. 70.

[10] Hassanlourad, M., Salehzadeh, H. and Shahnazari H. (2009), "Strength of Chemically Grouted Micro Pile Model in Calcareous Sand", 17th International Conference on Soil Mechanics & Geotechnical Engineering (ICSMGE), Alexandria, Egypt, 5-9 October.

[11] Hassanlourad, M., Salehzadeh, H. and Shahnazari H. (2010),"Mechanical Properties of Ungrouted and Grouted Carbonate Sands", International Journal of Geotechnical Engineering Vol. 4, pp. 507-516.

[12] Huang, J.T. and Airey, D.W. (1998), "Properties of Artificially Cemented Carbonate Sand", Journal of Geotechnical and Geoenviromental Engineering, ASCE, Vol. 124, No. 6. pp. 492-499.

[13] Ismail, M.A., Joer, H.A., Merit, A., and Randolph, M.F. (2002), "Cementation of Porous Material Using Calcite", Geotechnique, Vol. 52, No. 5, pp. 313-324.

[14] Ismail, M.H., Joer, H.A., Sim, W.H., and Randolph, M.F., (2002), "Effect of Cement Type on Shear Behavior of Cemented Calcareous Soil" Journal of Geotechnical and Geoenviromental Engineering, Vol. 128, No. 6, pp. 520-529.

[15] Lade, P.V., and Overton, D.D. (1989), "Cementation Effects in Frictional Materials", Journal of Geotechnical Engineering, ASCE, Vol. 115, No. 10, pp. 1373-1387.

[16] Salehzadeh, H. and Ghazanfari, E., (2004) "Parametric study of Kish carbonate sand under triaxial shearing", International Journal of Civil Engineering, Vol. 2, No. 4 , pp. 223-231.

[17] Salehzadeh, H, Hassanlourad, M., Procter, D.C. and Merrifield, C.M. (2008), "Compression and Extension Monotonic Loading of a carbonate Sand", International Journal of Civil Engineering, Vol. 6, No. 4 , pp. 266-274.

[18] Salehzadeh, H., Procter, D.C. and Merrifield, C.M. (2005) "A carbonate sand particle crushing under monotonic loading", International Journal of Civil Engineering, Vol. 3, No. 3, pp. 140-151.

[19] Saxena, S.K. & Lastrico, R.M. (1978), "Static Properties of Lightly Cemented Sand", Journal of Geotechnical Engineering, ASCE, Vol. 104, pp. 1449-1463.